

Characterization of pit formation in III-nitrides grown by metalorganic chemical vapor deposition

H. K. Cho, J. Y. Lee, and G. M. Yang

Citation: *Appl. Phys. Lett.* **80**, 1370 (2002); doi: 10.1063/1.1454215

View online: <http://dx.doi.org/10.1063/1.1454215>

View Table of Contents: <http://apl.aip.org/resource/1/APPLAB/v80/i8>

Published by the [American Institute of Physics](#).

Additional information on *Appl. Phys. Lett.*

Journal Homepage: <http://apl.aip.org/>

Journal Information: http://apl.aip.org/about/about_the_journal

Top downloads: http://apl.aip.org/features/most_downloaded

Information for Authors: <http://apl.aip.org/authors>

ADVERTISEMENT



Goodfellow
metals • ceramics • polymers • composites
70,000 products
450 different materials
small quantities fast

www.goodfellowusa.com

Characterization of pit formation in III-nitrides grown by metalorganic chemical vapor deposition

H. K. Cho^{a)} and J. Y. Lee^{b)}

Department of Materials Science and Engineering, Korea Advanced Institute of Science and Technology, 373-1 Gusong-dong, Yusong-gu, Daejeon 305-701, Korea

G. M. Yang

Department of Semiconductor Science and Technology and Semiconductor Physics Research Center, Chonbuk National University, Duckjin-Dong, Chunju 561-756, Korea

(Received 31 October 2001; accepted for publication 18 December 2001)

Pit formation in III-nitride heterostructures such as InGaN/GaN and AlGaIn/GaN grown by metalorganic chemical vapor deposition was characterized by transmission electron microscopy. The pit formation related with V defects has been reported in the InGaIn/GaN multiple quantum well with high In composition [Appl. Phys. Lett. **79**, 215 (2001)]. In this letter, we found that the mechanism of pit formation strongly depends on the indium and aluminum compositions in $\text{In}_x\text{Ga}_{1-x}\text{N}$ and $\text{Al}_x\text{Ga}_{1-x}\text{N}$ layers, respectively. By increasing the indium composition, the origin of pits is changed from the vertex of threading dislocations to the stacking mismatch boundaries induced by stacking faults and the three-dimensional island growth at the initial stage due to the large lattice mismatch. By increasing the aluminum composition, the origin of the pits also varied from the surface undulation due to the elastic misfit strain to the vertex of threading dislocations. In addition, several inversion domains observed in III nitrides result in pit formation in the surface of films. © 2002 American Institute of Physics. [DOI: 10.1063/1.1454215]

Nitride alloys (GaN, AlGaIn, and InGaIn) are promising semiconductors which have applications in both electronic devices operating at high temperature, high frequency, and high power and optical devices including light-emitting diodes in the blue-green and ultraviolet wavelength region.^{1,2} For $\text{In}_x\text{Ga}_{1-x}\text{N}$ and $\text{Al}_x\text{Ga}_{1-x}\text{N}$ layers grown on GaN, an increase in the indium (In) and aluminum (Al) compositions may inevitably cause misfit strains in films. Beyond a critical thickness, several structural defects such as misfit dislocations, stacking faults, V-shaped pits, etc., are generated by plastic relaxation.³ However, also at smaller thicknesses, elastic relaxation may be induced by the formation of islands, surface undulation, etc., as observed in InGaP/InAsP, $\text{In}_{0.77}\text{Ga}_{0.23}\text{As}/\text{InGaAs}$, SiGe/Si, and so on.⁴⁻⁶

Recently, we reported two models of the formation of V-shaped pits in InGaIn/GaN multiple quantum wells (MQWs) with high In composition.⁷ Also, the undesirability and the effect on the emission properties of these pits were previously demonstrated by transmission electron microscopy (TEM), cathodoluminescence, and photoluminescence.^{3,8,9} For the suppression of pit formation, therefore, a clear understanding of the mechanisms of pit formation is needed and the microstructure of the pits observed in various III-nitride films grown on sapphire substrate must be evaluated in detail. In this work, we investigated the pit formation originating from different sources in InGaIn/GaN and AlGaIn/GaN heterostructures with various In and Al compositions using TEM.

All samples were grown on *c*-plane sapphire substrates with a nominal 25 nm thick GaN nucleation layer by a hori-

zontal metalorganic chemical vapor deposition reactor operating at low pressure. Trimethylgallium, trimethylindium, trimethylaluminum, and ammonia were used as the source precursors for Ga, In, Al, and N, respectively. In order to analyze the effect of the strain on the mechanism of pit formation in III-nitrides, thick $\text{In}_x\text{Ga}_{1-x}\text{N}$ layers ($\sim 800 \text{ \AA}$) were grown at temperatures ranging from 830 °C ($x_{\text{In}} = 35\%$) to 880 °C ($x_{\text{In}} = 10\%$) and thick $\text{Al}_x\text{Ga}_{1-x}\text{N}$ layers ($\sim 1000 \text{ \AA}$) were grown at 1040 °C after growing the Si-doped underlying GaN layer of $\sim 2 \mu\text{m}$ thickness at 1080 °C. The In and Al compositions in the $\text{In}_x\text{Ga}_{1-x}\text{N}$ and $\text{Al}_x\text{Ga}_{1-x}\text{N}$ layers were 10%, 13%, 19%, and 35% and 16%, 25%, 44%, and 54%, respectively. Also, in order to investigate the effect of inversion domains on pit formation in III-nitrides, the MQWs composed of ten periods of InGaIn/GaN were grown on a GaN buffer layer of $\sim 2 \mu\text{m}$ thickness, and the Mg-doped AlGaIn layer and the 50 periods superlattice of AlGaIn (Mg-doped)/GaN were grown on *c*-plane sapphire substrates.

In order to characterize the pit formation of III-nitrides, TEM specimens were prepared in cross section along $[1\bar{1}20]$ zone axis using Tripod mechanical polishing followed by low temperature Ar ion milling at 4.5 kV in a Gatan DuoMill 660 DIF with sector speed control. The ion energy was gradually reduced during the final stages of thinning to minimize the surface damage of samples. Bright-field (BF) images and high-resolution TEM (HRTEM) images were recorded on a JEOL JEM-2000EX TEM at 200 kV and JEOL JEM-3010EX at 300 kV.

Figure 1 shows the cross sectional BF TEM micrographs from the $\text{In}_x\text{Ga}_{1-x}\text{N}$ layers grown with various In compositions on the GaN buffer layer. The theoretical critical In composition on the formation of the misfit dislocation of the $\sim 800 \text{ \AA}$ $\text{In}_x\text{Ga}_{1-x}\text{N}$ grown on GaN layers is less than 5%,

^{a)}Electronic mail: chohk@kaist.ac.kr

^{b)}Electronic mail: jylee@mail.kaist.ac.kr

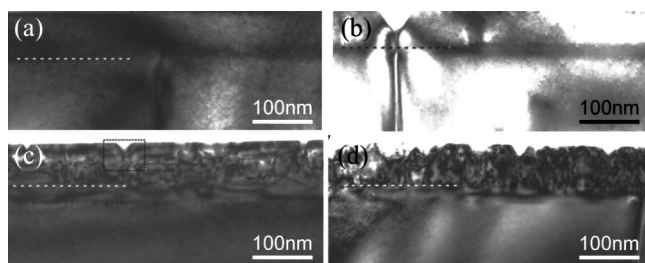


FIG. 1. Cross sectional BF TEM images using $g = 0002$ from the $\text{In}_x\text{Ga}_{1-x}\text{N}$ layers grown with the In composition of (a) 10%, (b) 13%, (c) 19%, and (d) 35% on the GaN buffer layer. The dashed lines indicate the $\text{In}_x\text{Ga}_{1-x}\text{N}/\text{GaN}$ interface.

below which the InGaN layers show coherent growth.¹⁰ Therefore, we expect the In composition of all $\text{In}_x\text{Ga}_{1-x}\text{N}$ layers studied here to have a value more than the critical In composition on the formation of the misfit dislocation. For $\text{In}_{0.1}\text{Ga}_{0.9}\text{N}/\text{GaN}$, no structural defects such as misfit dislocations, stacking faults, pits, etc., were observed within the $\text{In}_{0.1}\text{Ga}_{0.9}\text{N}$ layer. With a further increase in the In composition of the $\text{In}_x\text{Ga}_{1-x}\text{N}$ layer ($x_{\text{In}} = 13\%$), the V-shaped pits are generated to relax the stored misfit strain, as reported previously.^{8,11} It has been reported that a V-shaped pit is always connected with a threading dislocation from the GaN buffer layer at the bottom and only a small fraction of the threading dislocations causes the formation of the V-shaped pits in the InGaN layers and the InGaN/GaN MQWs.^{8,11} However, the density of V-shaped pits in the $\text{In}_{0.19}\text{Ga}_{0.81}\text{N}$ layer in Fig. 1(c) has a larger value than the threading dislocation density in the GaN buffer layer, which indicates that the formation of V-shaped pits in the InGaN with high In composition has a different origin, as reported previously for the InGaN/GaN MQW systems.⁷ We reported that in the InGaN/GaN MQWs with high In composition ($\sim 30\%$ In composition), most of the V-shaped pits are generated from stacking mismatch boundaries induced by stacking faults.⁷ Although the $\text{In}_{0.19}\text{Ga}_{0.81}\text{N}/\text{GaN}$ used here has an In composition of less than 20%, the part of V-shaped pits originate from stacking mismatch boundaries induced by stacking faults due to the increased InGaN layer thickness [Fig. 2(a)] compared to the InGaN/GaN MQW. For $\text{In}_{0.35}\text{Ga}_{0.65}\text{N}/\text{GaN}$, V-shaped pits with a density of more than 10^{10} cm^{-2} are observed on the surface. Unlike the pits in the $\text{In}_{0.19}\text{Ga}_{0.81}\text{N}/\text{GaN}$ sample, the $\text{In}_{0.35}\text{Ga}_{0.65}\text{N}$ regions with flat (0001) top surfaces between pits have a large number of

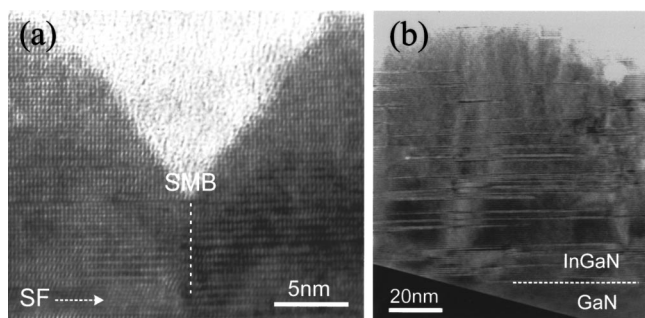


FIG. 2. (a) HRTEM image obtained from the dashed rectangle in Fig. 1(c). The observed V-shaped pit has a stacking fault on its lower position. (b) HRTEM image obtained from the $\text{In}_{0.35}\text{Ga}_{0.65}\text{N}$ on the GaN buffer layer.

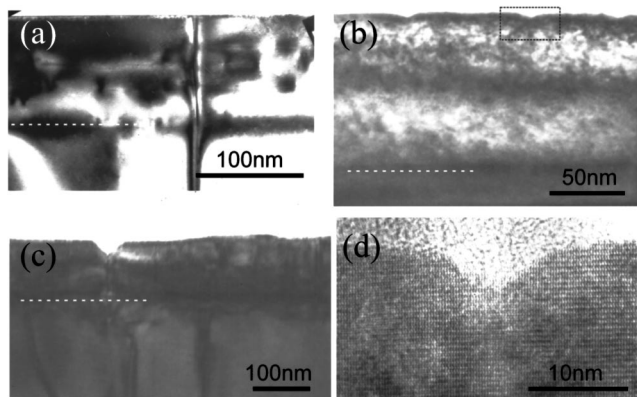


FIG. 3. Cross sectional BF TEM images using $g = 0002$ from the $\text{Al}_x\text{Ga}_{1-x}\text{N}$ layers grown with the Al composition of (a) 16%, (b) 44%, and (c) 54%. (d) HRTEM image obtained from the dashed rectangle in (b). The dashed lines indicate the $\text{Al}_x\text{Ga}_{1-x}\text{N}/\text{GaN}$ interface.

stacking faults and stacking mismatch boundaries formed at the initial growth stage of InGaN [Fig. 2(b)], that is, columnar structures including stacking faults. To relax the large lattice mismatch between $\text{In}_{0.35}\text{Ga}_{0.65}\text{N}$ and GaN, the initial $\text{In}_{0.35}\text{Ga}_{0.65}\text{N}$ layer was grown with the morphology of three-dimensional (3D) faceted islands.¹² A high density of stacking faults is clearly seen in the islands and the boundaries between subgrains by islands are visible like the growth of a GaN nucleation layer grown on sapphire substrate.¹³ Therefore, we think the pits in the $\text{In}_{0.35}\text{Ga}_{0.65}\text{N}/\text{GaN}$ sample are caused by such a 3D growth due to the lattice misfit at the initial growth of the InGaN layer.

As a result, we classified the origin of pit formation in the $\text{In}_x\text{Ga}_{1-x}\text{N}$ grown on the GaN buffer layer into three models as shown in Figs. 4(a), 4(b), and 4(c). For the $\text{In}_x\text{Ga}_{1-x}\text{N}$ layer with low In composition, pits are generated at the vertex of threading dislocations [Fig. 4(a)]. For the $\text{In}_x\text{Ga}_{1-x}\text{N}$ layer with medium In composition, pits are mainly generated from the stacking mismatch boundaries induced by stacking faults [Fig. 4(b)]. A further increase in In composition of the $\text{In}_x\text{Ga}_{1-x}\text{N}$ layer results in the 3D island growth at the initial stage and pit formation at the continuous growth [Fig. 4(c)].

To investigate the effect of Al composition on pit formation, cross sectional BF TEM micrographs from the $\text{Al}_x\text{Ga}_{1-x}\text{N}$ layers grown with various Al compositions on the GaN buffer layer were obtained as shown in Fig. 3. The theoretical critical Al composition on the formation of the misfit dislocation in the $\sim 1000 \text{ \AA}$ $\text{Al}_x\text{Ga}_{1-x}\text{N}$ layer grown on GaN layers is less than 15%.¹⁰ No pits are detected in the $\text{Al}_x\text{Ga}_{1-x}\text{N}$ layers with up to 25% Al composition. Only stacking faults and cracks in the AlGaIn layers are observed due to the misfit strain and the thermal coefficient difference, respectively (not shown). For the $\text{Al}_{0.44}\text{Ga}_{0.56}\text{N}/\text{GaN}$ sample, however, the surface of the $\text{Al}_{0.44}\text{Ga}_{0.56}\text{N}$ layer shows many pits that are not associated with structural defects such as threading dislocations, stacking faults, and so on [Figs. 3(b) and 3(d)]. The size of these pits is very small, an average diameter of 7 nm and an average height of ~ 3 nm, compared to that of pits in InGaN layers grown on GaN.^{7,8,10} It is believed that the formation of pits in $\text{Al}_{0.44}\text{Ga}_{0.56}\text{N}/\text{GaN}$ can be ascribed to the surface undulation by the increased elastic misfit strain as observed in III-V and II-VI semiconductor

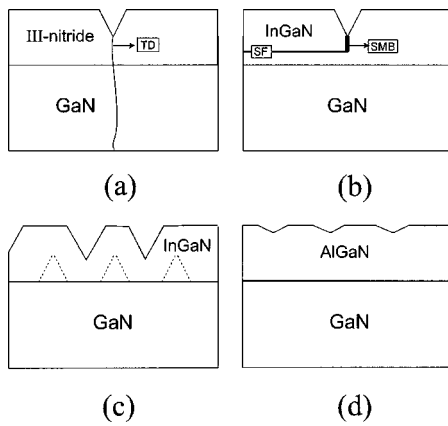


FIG. 4. Schematic models for pit formation related with (a) a threading dislocation observed in InGaN/GaN and AlGaIn/GaN heterostructures, (b) a stacking mismatch boundary induced by stacking faults and (c) the 3D island growth at the initial stage observed in an InGaN/GaN heterostructure, and (d) the surface undulation due to the elastic misfit strain observed in an AlGaIn/GaN heterostructure.

systems.^{4,5} The pit density is more than 10^{10} cm^{-2} in the surface. On the other hand, misfit dislocations are generated at the interface of the $\text{Al}_{0.54}\text{Ga}_{0.46}\text{N}/\text{GaN}$ sample in order to plastically relax the stored misfit strain as shown in Fig. 3(c). Also, V-shaped pits associated with threading dislocations at their bottoms are observed like InGaN/GaN heterostructures. These V-shaped pits have an open hexagonal, inverted pyramid with $\{10\bar{1}1\}$ sidewalls.^{8,10}

In consequence, we classified the origin of the pit formation in the $\text{Al}_x\text{Ga}_{1-x}\text{N}$ grown on the GaN buffer layer into two models as shown in Figs. 4(a) and 4(d). For the $\text{Al}_x\text{Ga}_{1-x}\text{N}$ layer with $\sim 40\%$ Al composition, pits are generated by the surface undulation due to the stored elastic misfit strain [Fig. 4(d)]. For the $\text{Al}_x\text{Ga}_{1-x}\text{N}$ layer with more than $\sim 50\%$ Al composition, however, pits are mainly generated at the vertex of threading dislocations [Fig. 4(a)] like InGaN/GaN.

Figure 5 is the cross sectional BF TEM micrographs showing the pits originating from inversion domains observed in various III-nitride heterostructures. Figures 5(a) and 5(b) demonstrate that IDBs generated from the GaN/substrate interface lead to pit formation at the surface. Unlike the pit formation by threading dislocations,^{8,10} however, the pit formation by IDBs does not disrupt the InGaN/GaN MQWs as shown in Fig. 5(a). The IDs observed near the surface area of nitride films with the AlGaIn (Mg-doped)/GaN superlattice also result in the pit formation due to the different growth rates within IDs compared to matrix around them as reported previously [Fig. 5(c)].^{14,15}

In summary, the pit formation in $\text{In}_x\text{Ga}_{1-x}\text{N}$ and $\text{Al}_x\text{Ga}_{1-x}\text{N}$ layers with various In and Al compositions grown on the GaN buffer layers was studied using TEM. We found that pits were formed from various origins such as threading dislocations, stacking mismatch boundaries, 3D is-

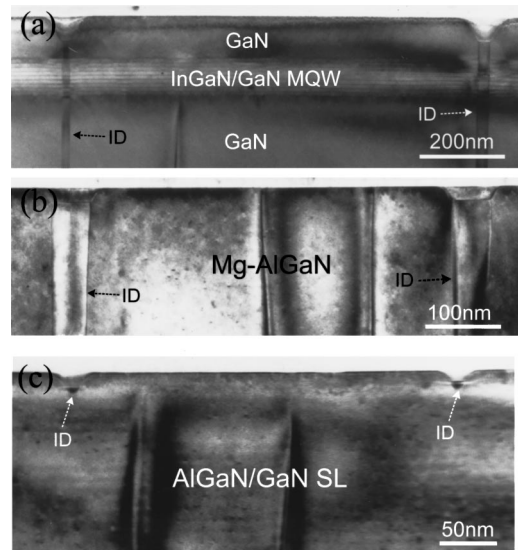


FIG. 5. Cross sectional BF TEM images using $g = 0002$ showing pit formation originating from inversion domain for (a) the InGaN/GaN MQW and (b) the Mg-doped AlGaIn layer. (c) Cross sectional BF TEM image using $g = 0002$ for the superlattice of AlGaIn (Mg-doped)/GaN showing pit formation by IDs observed near the surface.

land growth, surface undulation, and IDs depending on In and Al compositions.

This work has been supported by the Ministry of Science and Technology of Korea through the National Research Laboratory Program in Korea.

¹H. Morkoç, *Nitride Semiconductors and Devices* (Springer, Heidelberg, 1999).

²S. Nakamura, *Science* **281**, 956 (1998).

³H. K. Cho, J. Y. Lee, C. S. Kim, G. M. Yang, N. Sharma, and C. J. Humphreys, *J. Cryst. Growth* **231**, 466 (2001).

⁴P. Desjardins, H. Marchand, L. Isnard, and R. A. Masut, *J. Appl. Phys.* **81**, 3501 (1997).

⁵M. Mitsuhashi, M. Ogasawara, and H. Sugiura, *J. Cryst. Growth* **210**, 463 (2000).

⁶J. M. Hartmann, B. Gallas, J. Zhang, and J. J. Harris, *Semicond. Sci. Technol.* **15**, 370 (2000).

⁷H. K. Cho, J. Y. Lee, G. M. Yang, and C. S. Kim, *Appl. Phys. Lett.* **79**, 215 (2001).

⁸X. H. Wu, C. R. Elsass, A. Abare, M. Mack, S. Keller, P. M. Petroff, S. P. DenBaars, J. S. Speck, and S. J. Rosner, *Appl. Phys. Lett.* **72**, 692 (1998).

⁹G. Pozina, J. P. Bergman, B. Monemar, T. Takeuchi, H. Amano, and I. Akasaki, *J. Appl. Phys.* **88**, 2677 (2000).

¹⁰J. W. Matthews and A. E. Blakeslee, *J. Cryst. Growth* **32**, 265 (1976).

¹¹C. J. Sun, M. Z. Anwar, Q. Chen, J. W. Yang, M. A. Khan, M. S. Shur, A. D. Bykhovski, Z. Liliental-Weber, C. Kisielowski, M. Smith, J. Y. Lin, and H. X. Xiang, *Appl. Phys. Lett.* **70**, 2978 (1997).

¹²Z. Liliental-Weber, M. Benamara, J. Washburn, J. Z. Domagala, J. Bak-Misiuk, E. L. Piner, J. C. Roberts, and S. M. Bedair, *J. Electron. Mater.* **30**, 439 (2001).

¹³K. Lorenz, M. Gonsalves, Wook Kim, V. Narayanan, and S. Mahajan, *Appl. Phys. Lett.* **77**, 3391 (2000).

¹⁴L. T. Romano, M. Kneissl, J. E. Northrup, C. G. Van de Walle, and D. W. Treat, *Appl. Phys. Lett.* **79**, 2734 (2001).

¹⁵H. K. Cho, J. Y. Lee, S. R. Jeon, and G. M. Yang, *Appl. Phys. Lett.* **79**, 3788 (2001).